

1 **A Comparison of Machine Learning Methods**  
2 **for Predicting the Compressive Strength of Field-Placed Concrete**

3 *M.A. DeRousseau*<sup>1</sup>, *E. Laftchiev*<sup>2</sup>, *J.R. Kasprzyk*<sup>1</sup>, *B. Rajagopalan*<sup>1</sup>, *W.V. Srubar III*<sup>1,†</sup>

4 <sup>1</sup>Department of Civil, Environmental, and Architectural Engineering, University of Colorado Boulder,  
5 ECOT 441 UCB 428, Boulder, Colorado 80309-0428 USA,

6 <sup>2</sup>Mitsubishi Electric Research Labs, 201 Broadway FL8, Cambridge, MA 02139

7 <sup>†</sup>Corresponding Author, T +1 303 492 2621, F +1 303 492 7317, E [wsrubar@colorado.edu](mailto:wsrubar@colorado.edu)

8  
9 **Abstract**

10 This study evaluates the efficacy of machine learning (ML) methods to predict the compressive strength  
11 of field-placed concrete. We employ both field- and laboratory-obtained data to train and test ML models  
12 of increasing complexity to determine the best-performing model specific to field-placed concrete. The  
13 ability of ML models trained on laboratory data to predict the compressive strength of field-placed  
14 concrete is evaluated and compared to those models trained exclusively on field-acquired data. Results  
15 substantiate that the random forest ML model trained on field-acquired data exhibits the best performance  
16 for predicting the compressive strength of field-placed concrete; the RMSE, MAE, and  $R^2$  values  
17 were 730 psi, 530 psi, and .51, respectively. We also show that hybridization of field- and laboratory-  
18 acquired data for training ML models is a promising method for reducing common over-prediction issues  
19 encountered by laboratory-trained models that are used in isolation to predict the compressive strength of  
20 field-placed concrete.

21  
22 **Keywords:** concrete; compressive strength; machine learning; prediction; statistical modeling

23  
24 **1. Introduction**

25 The 28-day compressive strength of concrete is a critical design parameter for reinforced concrete  
26 structures [1]. Empirical prescriptive- and performance-based mixture design methodologies remain the  
27 conventional means to obtain concrete mixture design proportions that meet minimum 28-day  
28 compressive strength requirements. However, numerical approaches for predicting the 28-day  
29 compressive strength of concrete are emerging in the literature. Accurate numerical estimation of the 28-  
30 day compressive strength of concrete is desirable because more precise prediction (1) provides assurance  
31 of concrete quality, (2) reduces the number of concrete batches that are needed to be tested to meet  
32 strength targets, and (3) enables a reduction in factors of safety. Recent computational studies have  
33 demonstrated the ability of advanced statistical modeling techniques to numerically predict concrete  
34 compressive strength for laboratory-mixed concrete, termed *laboratory concrete* herein [2]–[13].

35 However, prediction of the 28-day compressive strength of concrete placed in the field on an actual  
36 construction site, termed *field concrete* herein, remains a challenge for the concrete industry due to  
37 variable environmental conditions and other uncertainties encountered during mixture proportioning,  
38 transport, placing, curing, and finishing.

### 39 *1.1 Prediction challenges for field concrete mixtures*

40 Estimating the 28-day compressive strength of concrete is a multifaceted problem. Complex physical and  
41 chemical interactions occur between concrete constituents, which, in turn, affect compressive strength.  
42 Therefore, nonlinear mathematical models are advantageous for accurately capturing all phenomena. As  
43 an example, consider the following physically intuitive correlations: compressive strength decreases  
44 (nonlinearly) as the water-to-cement ratio (w/c) increases [14], [15]; increasing air content for improved  
45 workability and freeze-thaw resistance also reduces compressive strength [16]. Other correlations have  
46 not been as intuitively deduced to-date. For example, it is well known that the proportion of coarse-to-fine  
47 aggregate affects compressive strength, but the relationship has not been precisely determined due to  
48 confounding factors, such as particle size distribution, aggregate angularity, and water demand. Coarse  
49 aggregate, for example, may vary in nominal size, grading, chemical composition, shape, surface texture,  
50 and absorptivity [17]; these properties can impact the strength of the interfacial bonds between the  
51 aggregate and mortar, which, in turn, affect the compressive strength of concrete. Furthermore, the  
52 addition of supplementary cementitious materials (SCMs), like fly ash, slag, and silica fume, also  
53 introduce new, complex, and nonlinear relationships to compressive strength because of complex factors,  
54 such as fineness, chemical variability, and pozzolanic reactivity [18], [19]. Additionally, the fineness and  
55 mineral composition of fly ash and slag can be highly variable, depending on the original industrial  
56 source and additional processing steps [20].

57 The conditions of the job site at which field concrete is mixed and placed are also highly variable and  
58 lead to high variability in field compressive strength compared to laboratory concrete. For instance, it is  
59 commonplace for the environmental conditions at construction sites to be loosely controlled. Here,  
60 temperature, humidity, and inclement weather can all affect concrete curing and the final compressive  
61 strength [21], [22]. Such variabilities do not exist in laboratory concrete mixing, which suggests that  
62 accurate prediction of the compressive strength of field concrete is a more challenging problem compared  
63 to compressive strength prediction of laboratory concrete.

### 64 *1.2 Machine learning methods for compressive strength prediction*

65 Because of the physical limitations described above, there is growing interest in predicting concrete  
66 compressive strength using machine learning (ML) models for both field and laboratory concrete  
67 mixtures [23], [24]. ML models predict compressive strength (*i.e.*, the target variable) from the types and  
68 quantities of the mixture ingredients (*i.e.*, the input variables). Using pairs of data of the form [input

69 variables, target variable], a model is trained from a collected dataset and learns the relationship between  
70 the target and input variables without constraint on prior intuitive understanding. The vast majority of this  
71 type of research has been performed on laboratory concrete, which, as discussed, suggests limitations on  
72 the actual usefulness of these models for predicting the compressive strength of field concrete, given the  
73 myriad of convoluting factors.

74 Prior research in ML methods for compressive strength prediction has been limited to testing ML  
75 methods using laboratory data to determine best-possible prediction models for concrete compressive  
76 strength. A particularly popular ML algorithm is artificial neural networks (ANNs). The first study of  
77 ANNs by Yeh *et al.* [25] employed ANNs on a dataset of over 1000 laboratory concrete mixture designs.  
78 Since then, other researchers have reported ANN studies with coefficients of determination ( $R^2$ ) of up to  
79 0.999 [2]–[8], [10], [26]–[28]. However, a significant number of ANN studies employ less than 100  
80 experimental data points, which may not sufficiently sample the predictor variable space. While ANNs  
81 are a flexible and powerful ML method, it suffers from the need to train a large number of parameters.  
82 For small datasets (as is common for field concrete), ANNs can quickly overfit the data, which leads to  
83 strong training set performance but poor generalization performance on new datasets. Other ML methods  
84 that appear in the literature include support vector machines (SVM) [25], [26] and decision tree-based  
85 models [13], [29]. Studies that employ these methods are less common than ANN studies, due to the  
86 historical alignment of compressive strength prediction and ML methods.

87 Some narrower-scope prediction studies that used ML have focused on modeling concrete mixtures  
88 that contain particular mixture ingredients, such as fly ash [28], blast-furnace slag [30], recycled  
89 aggregate [31], silica fume [32], and metakaolin [33]. This body of research generates models that are  
90 useful for predicting compressive strength when specific constituents are included. However, this  
91 approach narrowly tailors the model to the particular dataset and, thus, is less useful when either mixture  
92 ingredients or external conditions (possibly unmeasured) may change.

93 A recent study by Young *et al.* considered field concrete data and compared the predictive  
94 performance of four ML models for predicting both *field* and *laboratory concrete* [23]. This study found  
95 that variance can be significantly better explained in the laboratory concrete dataset, which is compatible  
96 with the idea that *laboratory concrete* has fewer uncontrolled variables. The study determined that the  
97 four ML methods investigated exhibited equivalent predictive performance for *field concrete* – a  
98 somewhat unintuitive result, given that the four methods employed do not share common assumptions  
99 about the underlying data. In addition, it is also of note that the laboratory and field datasets contained  
100 different mixture ingredients (*i.e.*, input variables). For example, the laboratory concrete dataset included  
101 blast-furnace slag, while the field concrete dataset did not, making an apples-to-apples comparison  
102 difficult between models for both laboratory and field concrete.

### 103 1.3. Innovative contribution/knowledge gaps

104 Despite a large body of research in this area of study, the challenge of training a ML model for accurate  
105 prediction of concrete compressive strength remains relevant. More specifically, two significant gaps  
106 exist in the literature. First, prior studies are not well-grounded in best-practice methods of the ML  
107 community. The standard procedure in ML is to generate a pipeline of methods that increase in  
108 complexity [34]. The reason for this is two-fold: (1) while powerful, ML methods often search a large  
109 model space and may miss simple solutions recognized by the researcher and (2) the failure of simpler  
110 models is typically caused by a failure in model assumptions that reveals previously hidden details about  
111 the data interactions and non-linear behavior observed in the system. These failures can thus be used to  
112 inform the appropriate choice of ML tools for further development. Second, consensus on the best model  
113 architectures for predicting the compressive strength of field concrete has not yet been reached.

114 To this end, this study aims to address the aforementioned knowledge gaps and is particularly focused  
115 on approaches for accurate prediction of the compressive strength of *field concrete*. First, we employ the  
116 standard ML procedure of testing models of increasing complexity in order to determine the best-  
117 performing model for field concrete. This procedure enables us to build on past research by discussing  
118 *why* certain ML methods are particularly well-suited for the concrete compressive strength prediction  
119 problem. The field concrete dataset in this study contains 1681 concrete mixtures and was collected by  
120 the Colorado Department of Transportation (CDOT). The laboratory concrete dataset in this study was  
121 obtained from the University of California, Irvine Machine Learning Repository, which contains data for  
122 more than 1000 mixtures [35].

123 Following the analysis of the field concrete models trained on the field concrete dataset, we evaluate  
124 the ability of ML models learned on laboratory concrete data to predict the compressive strength of field  
125 concrete mixtures. For this analysis, we perform the same ML procedures for the laboratory data and  
126 select the best-performing model. This model is then used to predict the compressive strength of field  
127 concrete mixtures, and the relative model performance is analyzed. It was hypothesized that the  
128 laboratory ML model performance would be unsatisfactory for predicting field compressive strength  
129 compared to that of models trained exclusively on field concrete data. Finally, this work includes an  
130 analysis of laboratory data-trained models that are supplemented with varying percentages of field data in  
131 order to determine if such hybridized datasets can improve performance the predictive capabilities of  
132 laboratory concrete models.

## 133 2. Machine Learning (ML) Methods

134 As discussed in the introduction, this paper builds a pipeline of ML methods with increasing complexity,  
135 such that the underlying structure in the training data can be stepwise analyzed. First, in Section 2.1, we  
136 describe the ML methods used in the pipeline. We introduce *linear methods* (*i.e.*, linear regression,

137 polynomial regression), *transformed linear methods* (i.e., kernelized support vector regression, kernelized  
 138 Gaussian process regression), and *non-linear methods* (i.e., regression trees, boosted trees, random  
 139 forest). In general, simple models are introduced first, and subsequent models increase in complexity. The  
 140 simplest methods (e.g., linear regression) tend to require the most assumptions about the underlying data  
 141 structure, and the most complex methods (e.g., boosted trees) require few assumptions about the  
 142 underlying structure of the data. Second in Section 2.2, we analyze the utility of predictive models trained  
 143 on laboratory concrete data for predicting field concrete strength. Third, in Section 2.3, we introduce the  
 144 performance measures used to evaluate the effectiveness of each model: the coefficient of determination  
 145 ( $R^2$ ), root mean squared error (RMSE), and mean absolute error (MAE). Last, in Section 2.4, overfitting is  
 146 discussed, which occurs when a model not only captures the desired qualities in the data, but also begins  
 147 to exactly model the training data itself. An overfitted model is undesirable because it lowers the  
 148 predictive performance on “unseen” testing data. In other words, overfitted models do not generalize well  
 149 to real-world cases. In this analysis, we describe and utilize nested cross-validation as a means reduce  
 150 overfitting. Reserved testing data is used for final determination of the best-performing model.

## 151 2.1 ML Methods

152 All models were created in the R Project for Statistical Computing [36]; in addition, Table 1 lists the ML  
 153 methods employed in this study, as well as the specific package and function used for model training. For  
 154 each ML method, we discuss parameter tuning and the intuitive meaning of the parameters.

155 **Table 1.** ML models and corresponding R packages used in this study.

Model Type	R Package	R Function
<i>Linear Methods</i>		
Linear regression	stats	lm
Polynomial regression	stats	lm
<i>Transformed Linear Methods</i>		
Kernelized support vector regression	kernlab	ksvm
Kernelized Gaussian process	kernlab	gausspr
<i>Non-Linear Methods</i>		
Regression trees	rpart	rpart
Random forest	randomForest	randomForest
Boosted trees	gbm	gbm

156

### 157 2.1.1 Linear Regression

158 The simplest model to apply and analyze is linear regression. In addition to providing useful  
 159 understanding of the data, linear regression also serves as a good baseline from which other techniques  
 160 can be evaluated. Linear regression is a model that describes the output (target) variable as a linear  
 161 combination of the predictor variables [37]. This linear combination is a hyperplane in N-dimensional  
 162 space, where N is the number of coefficients in the model. The model solution is the hyperplane that

163 minimizes the squared error between the observed output and the predicted output. Mathematically, the  
164 solution is described as:

$$165 \quad \hat{y} = \mathbf{x}^T \boldsymbol{\beta}, \quad \text{Eq. 1}$$

166 where  $\mathbf{x}$  is the input vector,  $\boldsymbol{\beta}$  is the N-dimensional vector of coefficients (parameters) for the linear  
167 model, and  $\hat{y}$  is the predicted output variable from the model. The underlying assumption in linear  
168 regression is that the relationship between the predictor variables and the output variable is linear.  
169 Moreover, the model assumes that predictor variables are independent from one another, and the resulting  
170 residuals, the difference between the predicted and observed output variables, are both homoscedastic  
171 (*i.e.*, have constant variance) and normally distributed. When these assumptions are violated, it indicates  
172 that a linear model is not appropriate. When such violations occur, it is reasonable to use transformations  
173 on the input data to try to reduce or eliminate the violation in assumptions. Failure of such methods to  
174 improve the resulting model error and reduce violation of the assumptions means that the dataset requires  
175 more complex non-linear models.

### 176 **2.1.2 Multivariate Polynomial Regression**

177 Multivariate polynomial regression (called *polynomial regression* in this study) uses nth degree  
178 polynomials of the input variables to predict the output variable. Polynomial regression is a generalization  
179 of Eq. 1; however, each  $x$  term may be: (1) an original predictor variable (*e.g.*,  $x_1$ ), (2) a pure higher-order  
180 term of one predictor variable (*e.g.*,  $x_1^4$ ), or (3) an interaction term between two or more predictor  
181 variables (*e.g.*,  $x_1x_2^2$ )

182 A generalized example of an expanded second-order polynomial solution with two predictor variables  
183 (for simplicity) is described by:

$$184 \quad \hat{y} = \beta_0 + \beta_1x_1 + \beta_2x_2 + \beta_{11}x_1^2 + \beta_{22}x_2^2 + \beta_{12}x_1x_2 \quad \text{Eq. 2}$$

185 The transformation of the predictor variables allows for modeling of higher-order relationships and  
186 modeling interactions between the input variables; Eq. 2, for example, shows a parabolic relationship.  
187 When the original predictor variables are transformed, they are called “features.” This term, also  
188 commonly applied to all input variables of the models, denotes the fact that the inputs have been  
189 transformed from their original space. In this analysis, polynomials up to third-order are employed, where  
190 third order is chosen due to limits in computational power. Since polynomial regression is a form of linear  
191 regression, the same assumptions are required—more specifically, independence of the input features,  
192 homoscedasticity of the residuals, and normality of the residuals. Note, however, these assumptions apply  
193 to the transformed features and not the original data space.

### 194 **2.1.3 Kernelized Regression Methods**

195 Kernalized regression methods utilize two mathematical concepts applied in tandem – a transformation of  
 196 the predictor variables and the pairing of the new predictors with a regression method. These pairings can  
 197 then be analyzed in order to determine which (if any) kernel and regression assumptions fit the data well.

198 Kernels are a set of transformations that can be used to map the original predictor variable space to a  
 199 high-dimensional feature space [34]. Here, this mapping is more complex than the polynomial mappings  
 200 in the previous section, and all mappings are the result of extensive previous research effort [38]. Each  
 201 kernel has its own set of *tuning parameters* that must be optimized. This paper compares four kernel  
 202 transformations, including: linear kernel, radial basis function (RBF) kernel, sigmoid kernel, and  
 203 polynomial kernels (up to order 4). The model order of the polynomial kernels is only limited by the  
 204 available computational power.

205 Kernel transformations have the form:

$$206 \quad k(\mathbf{x}, \mathbf{x}') = \langle \phi(\mathbf{x}), \phi(\mathbf{x}') \rangle \quad \text{Eq. 3}$$

207 where  $k$  is the kernel function,  $\mathbf{x}$  and  $\mathbf{x}'$  are N-dimensional input vectors (N is the number of predictor  
 208 variables), and  $\phi$  is a mapping from m dimensions to an m-dimensional space. Note that  $\langle \phi(\mathbf{x}), \phi(\mathbf{x}') \rangle$   
 209 denotes the inner product between the two mappings and can be thought of as a measure of similarity  
 210 between the two transformed vectors. The kernel tuning parameters are optimized in tandem with the  
 211 optimization of a regression model. This optimization is discussed below. Table 2 provides the kernel  
 212 transformation equations and kernel tuning parameters used in this study.

213 **Table 2.** Kernel Transformation equations and tuning parameters

Name	Kernel Transformation	Tuning Parameters
Linear	$k(\mathbf{x}, \mathbf{x}') = \langle \mathbf{x}, \mathbf{x}' \rangle$	n/a
Radial Basis Function	$k(\mathbf{x}, \mathbf{x}') = \exp(-\gamma \ \mathbf{x} - \mathbf{x}'\ ^2)$	$\gamma$
Polynomial	$k(\mathbf{x}, \mathbf{x}') = (\gamma \langle \mathbf{x}, \mathbf{x}' \rangle + r)^d$	$\gamma, r,$ and $d$

214  
 215 The transformed variables (features) can be utilized with any regression method. The concept here is that  
 216 parameters for both the kernel transformations and the regression methods are tuned simultaneously such  
 217 that the cross-validated model error is minimized. When there are multiple tuning parameters, a grid  
 218 search technique is employed in order to find near-optimal parameter values. In this paper, two kernalized  
 219 regression methods are tested: support vector regression and Gaussian process regression.

220 Support vector regression (SVR) is a version of support vector machines (SVM) used for regression  
 221 purposes (rather than classification) [39]. The regression model generated by SVR depends on only a  
 222 subset of the dataset, and these data points are deemed *support vectors*. When an SVR model is trained,  
 223 support vectors are the points from the dataset that produce error values ( $\epsilon$ ) larger than a prescribed

224 threshold value. SVR model training generates values for  $\beta_m$  (the coefficients for the transformed support  
 225 vectors) and  $\beta_0$  (the intercept). This occurs via minimization of Eq. 4 using gradient descent:

$$226 \quad \min: H(\beta_m, \beta_0) = \sum_{i=1}^N V(y_i - \hat{y}) + \frac{\lambda}{2} \sum \beta_m^2 \quad \text{Eq. 4}$$

227 Here,  $V(r)$  is the prescribed error measure,  $y$  is the observed target variable, and  $\lambda$  is a regularization  
 228 parameter that serves as a degree of importance given to large error values. When  $\lambda$  increases, large errors  
 229 are more greatly penalized in the model; this parameter can be tuned using cross-validation. In this study  
 230 the SVR is paired with the aforementioned kernel transformations in order to examine the utility of  
 231 transformations of the predictor variables.

232 The second regression method that is employed with the kernel-transformed data is Gaussian process  
 233 regression (GP). GP can be thought of as the Bayesian interpretation of linear regression. Rather than  
 234 assuming that the relationship between the predictor variables and the target variable has the prescribed  
 235 linear functional form (e.g.  $\hat{y} = \mathbf{x}^T \boldsymbol{\beta}$ ), GP simply assumes that the data can be represented as a sample  
 236 from a multivariate Gaussian distribution and that the mean of this distribution is zero. This approach is  
 237 “less parametric” in the sense that the model is more loosely defined. Using GP, the predictions of the  
 238 target variable are made using the conditional probability,  $p(y_* | \mathbf{y})$ . In short: given the data, how likely is  
 239 a certain prediction for  $y_*$ ? Here, note the subtle difference between  $\hat{y}$  and  $y_*$ .  $\hat{y}$  represents a predicted  
 240 target variable from a model, and  $y_*$  represents a distribution of possible outputs from the model. In the  
 241 case of GP,  $\hat{y}$  is the expected value of  $y_*$ ,  $E[y_*] = E[y_* | \mathbf{y}]$ .

242 Given the assumed Gaussian distribution, the matrix of all predictor variables in the dataset ( $\mathbf{X}$ ), the  
 243 output vector ( $\mathbf{y}$ ) and the new matrix of data inputs, the goal is to make a prediction on the new set of data  
 244 points ( $\mathbf{x}_*$ ). The derived conditional distribution has the form,

$$245 \quad y_* | \mathbf{y} \sim N(\mathbf{K}_* \mathbf{K}^{-1} \mathbf{y}, \mathbf{K}_{**} - \mathbf{K}_* \mathbf{K}^{-1} \mathbf{K}_*^T), \quad \text{Eq. 5}$$

246 where  $\mathbf{K}$ ,  $\mathbf{K}_*$ , and  $\mathbf{K}_{**}$  are the covariance matrices resulting from  $k(\mathbf{x}, \mathbf{x}')$ ,  $k(\mathbf{x}_*, \mathbf{x}')$ , and  $k(\mathbf{x}_*, \mathbf{x}_*')$ ,  
 247 respectively. The prediction,  $\hat{y}$ , is the expected value of this distribution, which can be reduced to the  
 248 equation below.

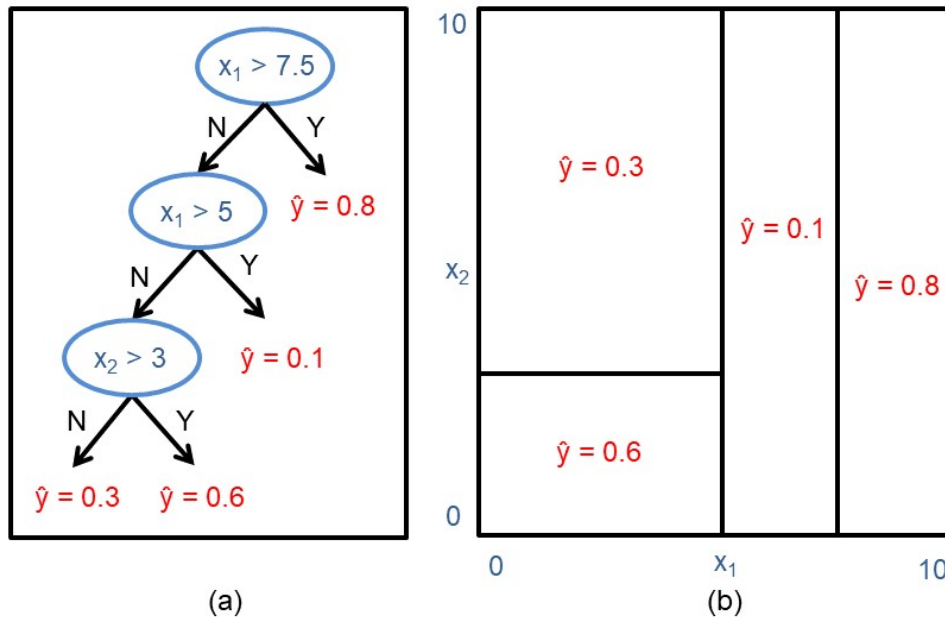
$$249 \quad \hat{y} = \mathbf{K}_* \mathbf{K}^{-1} \mathbf{y} \quad \text{Eq. 6}$$

250 Since GP employs only the assumption of a Gaussian distribution and the covariance matrices for model  
 251 formulation, no tuning parameters are necessary for this regression method beyond those required for the  
 252 choice of kernel. The performance of GP allows us to assess the veracity of the Gaussian distribution  
 253 assumption for the data under multiple different transformations of the predictor variables. If none of the  
 254 above regression methods can adequately model the output variable, models with no linearity assumptions  
 255 (e.g. regression trees, artificial neural networks) are reasonable model options consider.



256 **2.1.4 Regression Trees**

257 The goal of a regression tree is to generate partitions in the predictor variables such that the target variable  
 258 can be predicted based on the partitions among the input variables. Figure 1a provides a simple  
 259 illustration of regression tree “nodes” (*i.e.*, partition rules) and “leaves” (*i.e.*, terminal nodes that lead to  
 260 one output value). For instance, in the example provided in Figure 1a, there are two predictor variables ( $x_1$   
 261 and  $x_2$ ). The “root node” (the uppermost blue ellipse) is a rule that partitions the data along  $x_1$ . For this  
 262 node, if  $x_1$  is greater than 7.5, then the predicted output (in red) is 0.8. However, if the value of  $x_1$  is less  
 263 than 7.5, then one must proceed to the next node in the tree. This process continues until a predicted  
 264 output variable is reached. For the same example regression tree, Figure 1b demonstrates that a regression  
 265 tree partitions the predictor variables into rectangular spaces; the and the predicted output is the same  
 266 value throughout each of these rectangular cells.



267

268 **Figure 1: (a)** Diagram of an example regression tree model with two predictor variables,  $x_1$  and  $x_2$ . **(b)**  
 269 This diagram shows the same decision tree using the two predictor variables as axes. It helps visualized  
 270 the rectangularity of the target variable predictions when simple regression trees are employed. Within  
 271 each rectangle the predicted target variable would be the same.

272 Training a regression tree is performed by selecting partitions in succession using a criterion of  
 273 variance reduction in the target variable [40]. Since each successive partition is always chosen such that  
 274 the variance of the target variable is reduced, regression trees are prone to overfitting the data. To prevent  
 275 overfitting, a variety of regularization techniques can be employed. This study minimizes the cost

276 complexity function, which places a penalty for each additional node that is selected for the model. As  
277 shown below, the cost complexity function  $R_\alpha(T)$  has two terms that influence its value:

$$278 \quad R_\alpha(T) = R(T) + \alpha * f(T), \quad \text{Eq. 7}$$

279 where  $R(T)$  is the training error,  $f(T)$  is the number of leaves in the regression tree, and  $\alpha$  is the  
280 regularization parameter that is determined via cross-validation [41]. In Section 2.3 the cross-validation  
281 procedure used in this study is thoroughly discussed.

282 Regression trees have the advantage that they do not assume linearity in the data, and, therefore, no  
283 complex data transformations are needed. Overall, this approach is simpler than linear methods, but it  
284 requires careful consideration so as not to overfit the data. Regression trees also implicitly select  
285 variables, which means that a trained regression tree will show variables that have more importance for  
286 predicting the target variable in earlier nodes in the tree. Lastly, regression trees are interpretable and can  
287 provide some insight on the dataset being analyzed.

288 A disadvantage of simple regression trees is that they suffer from model instability; in other words,  
289 small changes to the dataset might create a completely different set of partitions, and, consequently does  
290 not lead to the best-performing model. For this reason, more complicated tree-based methods are often  
291 considered that are more stable. Random forest and boosted trees are examples of more complex tree-  
292 based methods that aim to reduce this instability and are discussed in the subsequent sections.

### 293 **2.1.5 Random Forest**

294 Random forest is a method that builds an ensemble of regression trees in order to reduce the instability of  
295 individual trees. Random forest utilizes two strategies for improving the instability issue. First, it employs  
296 the concept of “bootstrap aggregation” (sampling with replacement) in order to generate many similar  
297 datasets that were sampled from the same original dataset. These datasets each lead to an individual tree  
298 within the ensemble. Second, it incorporates randomness during tree-learning in order to reduce the  
299 correlation between each tree within the ensemble. For instance, when generating new nodes (for  
300 individual trees within the random forest), only a subset of the original predictor variables is selected as  
301 the set of candidate variables on which to partition the data. The variable value that minimizes variance in  
302 the output from these randomly selected predictors is the variable selected for that node. This process is  
303 repeated for all nodes in a regression tree and then for all regression trees in the random forest. For a  
304 random forest model, the tuning parameters are: the number of randomly selected predictors ( $k$ ), the  
305 number of individual trees that are trained ( $n$ ), and the tree depth ( $d$ ) [42].

306 The advantage of the random forest method is that it significantly reduces the instability of simple  
307 regression trees. Furthermore, this method has been shown to minimize correlation between trees  
308 compared to other tree-ensemble methods (e.g. “bagging trees” that use only bootstrap aggregation and

309 not random variable selection) [40]. One disadvantage of random forests is their reduction in  
310 interpretability compared to simple regression trees; random forests cannot be easily visualized and  
311 individual trees are often not good predictive models on their own. However, variable importance plots  
312 can reveal the relative importance of predictor variables.

### 313 **2.1.6 Boosted Trees**

314 Like random forest, boosted trees are an ensemble method for dealing with the instability and poor  
315 predictive performance of simple regression trees. Generally, the concept of “boosting” is an ensemble  
316 strategy that can be used to improve weak learning algorithms (e.g. regression trees) [43], [44]. Boosting  
317 can be applied to any weak learning algorithm but is commonly utilized for regression trees. The main  
318 concept of boosting is to build a model using the weak learning algorithm. Then another model is learned  
319 on the *residuals* from the first model. This step of model-building on the previous model’s residuals is  
320 repeated for a set number of iterations. Therefore, a boosted tree is simply a model where the weak  
321 learning algorithm used in each iteration is a regression tree.

322 Unlike random forest in which all trees are of the same importance, boosted trees are hierarchical,  
323 meaning that each tree layer is constructed recursively. The tuning parameters for boosted trees are: the  
324 number of trees, the interaction depth (maximum number of nodes per tree), the minimum number of  
325 observations per node (a stopping criteria used to prevent trees that have only one observation at each  
326 leaf), and the shrinkage rate (the rate at which the impact of each additional tree is reduced).

327 Boosted trees are similar to random forest in their advantages and disadvantages. Boosted trees tend to  
328 have high predictive performance on highly nonlinear datasets and can be successful on problems where  
329 there is unequal importance of predictor variables [34]. One disadvantage of boosted trees is that this  
330 method has low interpretability; it is difficult to gain much intuition of the patterns that the model has  
331 learned or to determine why a boosted tree model is successful (or not) at predicting the target variable.  
332 This means that a strong ML pipeline must be used to train boosted trees to ensure that the approach has  
333 not overfit the data.

334

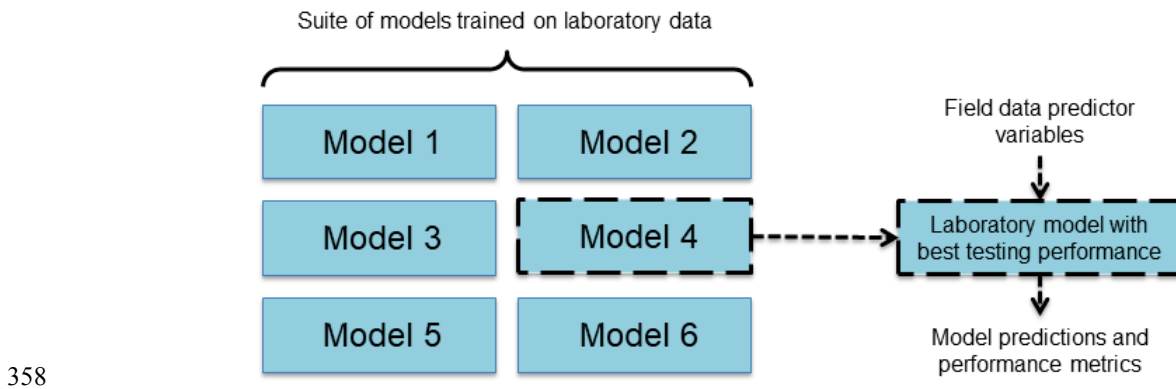
## 335 *2.2 Testing of Laboratory and Hybrid Models for Field Concrete Strength Prediction*

### 336 **2.2.1 Laboratory Models**

337 As was discussed in the introduction, many studies in the literature have developed ML models for  
338 predicting concrete compressive strength using laboratory concrete datasets. While these laboratory  
339 models report high predictive performance [2], [4]–[8], [10], [26], [27], it has not yet been tested whether  
340 they are useful for predicting the compressive strength of field concrete. A significant novelty of this  
341 study is that laboratory models are tested to determine if they are, in fact, useful for predicting  
342 compressive strength when presented with other datasets – namely, field concrete data.

343 One issue preventing the direct testing of laboratory ML models from the literature is the use of  
344 concrete age as a predictor variable. In other studies, age is a convenient predictor variable because it can  
345 explain a high percentage of variance in compressive strength data. In other words, removing age as a  
346 predictor and using only the final compressive strength as the output causes the compressive strength  
347 problem to be significantly more difficult (*i.e.*, model performance measures tend to be poorer). In this  
348 analysis, the desired model output is the final compressive strength (approximated by the 28-day strength)  
349 of a concrete mixture as a function of only the quantities of the mixture ingredients. Due to this difference  
350 between the prediction problem described herein and that of the literature, laboratory models for  
351 predicting the 28-day compressive strength using laboratory concrete data have been trained specifically  
352 for this study. Model utility is examined via the process described below and illustrated in Figure 2.

353 First, the aforementioned suite of ML models (*i.e.*, linear regression, polynomial regression, kernel  
354 regression, tree-based models) is trained and tested using the laboratory data described in Section 3. The  
355 model with the best testing performance is selected. Then, the predictor variables from the field data are  
356 used as inputs and the performance measures and diagnostic plots for this new data shall be reported and  
357 analyzed.



358  
359 **Figure 2.** Process for testing the predictive capability of laboratory models using field concrete data. The  
360 dotted outline indicates the laboratory model that is selected based on its performance measures.

### 361 2.2.2 Models Trained on Hybrid Data

362 It was hypothesized that the previously-described laboratory model will not satisfactorily predict the  
363 compressive strength of real concrete mixtures. Thus, an analysis of models trained on hybrid data (*i.e.*, a  
364 dataset that is composed of both field laboratory data) is conducted to determine whether they can  
365 improve predictive performance compared to “pure” laboratory models.

366 Models trained on hybrid data are potentially valuable because there is an inherent tradeoff between  
367 the use of laboratory and field models for predicting real concrete compressive strength. On one hand,  
368 laboratory data is the cheapest and most accessible data to acquire. It is also the best method for exploring

369 new and exotic concrete mixtures that are uncommon in industry. However, laboratory compressive  
370 strength data has the disadvantage that it does not reflect the full set environmental variables experienced  
371 by field concrete. Accordingly, it is expected that ML models trained on hybrid data may have the  
372 potential to improve the predictive performance of laboratory models.

373 In this novel hybrid approach, a percentage,  $\alpha$ , of the hybrid dataset is composed of the field data, and  
374 the rest is composed of the laboratory dataset. This procedure is used to determine if small amounts of  
375 field data can improve model performance. In order to determine the effect of variable amounts of field  
376 data, different  $\alpha$  values are utilized (10%, 20%, 30%, 40%, and 50%). The model building process occurs,  
377 as follows, for each value of  $\alpha$ :

378 For each  $\alpha$ :

- 379 1. Sort the field dataset in the order of lowest compressive strength to highest compressive strength  
380 and partition this sorted dataset into quintiles.
- 381 2. In order to ensure the field data portion of the hybrid data is well-sampled, randomly sample (in  
382 equal number) the appropriate number for points from the quintiles of the sorted field dataset.  
383 Randomly sample from the field dataset the appropriate number of points.
- 384 3. Use this hybrid data to train a cross-validated ML model. (The selection of ML model is  
385 determined by the best performing laboratory model.)
- 386 4. Use the remaining, unsampled field data to determine the average testing performance of the  
387 hybrid model. The performance measures described in the following section are reported.
- 388 5. Repeat steps 1-4 five times to find average performance measures for each  $\alpha$ .

### 389 *2.3 Performance Measures*

390 When training statistical, data-driven models, it is necessary to have a method to quantify the model  
391 performance so that hyperparameter tuning can be iterated to select the best possible model. There are  
392 several established metrics for determining predictive performance, each with advantages and  
393 disadvantages, which will be discussed below. Common quantitative performance measures common to  
394 regression modeling (rather than classification modeling) include the coefficient of determination ( $R^2$ ),  
395 root mean square error (RMSE), and mean absolute error (MAE) [45], [46]. These metrics, coupled with  
396 model diagnostic plots and visualization of predicted versus observed output values, provide a  
397 comprehensive picture of a model's performance.

398  $R^2$  is a measure of the proportion of the variance in the data that is explained by the model.  
399 Accordingly,  $R^2$  is the ratio shown in Eq. 8, where  $y_i$  is the observed value from the data,  $\hat{y}_i$  is the  
400 predicted value from the model, and  $\bar{y}$  is the average output from the data.

$$401 \quad R^2 = \frac{\sum_i (\hat{y}_i - \bar{y})^2}{\sum_i (y_i - \bar{y})^2} \quad \text{Eq. 8}$$

402 The value of  $R^2$  ranges from zero to one, with higher values indicating a better ability to explain the  
403 variance in the data with the model. However,  $R^2$  is a measure of correlation, not accuracy, and should be  
404 used with other performance measures because it is dependent on the variance of the output variable.

405 The root mean square error (RMSE) indicates how concentrated the data is around the model fit. The  
406 RMSE is measured on the same scale as the output variable, and is always positive due to the squared  
407 residuals in its calculation. Using the RMSE accentuates the effect of outliers in the error metric. This  
408 means that if median error of the model (usually captured by the mean absolute error) is low, the RMSE  
409 of the model can still be large due to the inability to model some outliers in the data. Given observed  
410 values,  $y_i$ , predicted values,  $\hat{y}_i$ , and  $n$  observed values RMSE is calculated as:

$$411 \quad RMSE = \sqrt{\frac{\sum_{i=1}^n (\hat{y}_i - y_i)^2}{n}} \quad \text{Eq. 9}$$

412 The mean absolute error (MAE) is a measure of prediction accuracy of a model that uses the absolute  
413 value of the errors rather than a squared value. The use of the absolute value reduces the influence of very  
414 large errors on the measure of performance. Thus, MAE is a measure of the median error of the model  
415 and is complimentary to the use of  $R^2$  and RMSE.

$$416 \quad MAE = \frac{\sum_{i=1}^n |\hat{y}_i - y_i|}{n} \quad \text{Eq. 10}$$

417 Like RMSE, MAE is measured on the same scale as the output variable, and a lower value indicates a  
418 better model fit. In addition, MAE values for a model are typically smaller than the RMSE value for the  
419 same model. In this paper we chose to use both RMSE and MAE in order to report both the median and  
420 mean error of each model.

#### 421 2.4 Cross-validation

422 A critical issue to consider when training and comparing statistical and machine learning models is the  
423 prevention of *overfitting*. Overfitting is a problem for ML models that have a high capacity to learn non-  
424 linear relationships and are trained on datasets that do not contain a sufficiently large variance of the data  
425 (*i.e.*, on datasets that are not rigorously sampled). When using iterative training methods such as grid  
426 search, a model is particularly prone to overfitting if the same data is used for the training and validation  
427 datasets. In this case, the resulting performance measures would indicate that the model has good  
428 predictive performance, but when these models are tested on new data, poor performance is observed.

429 To prevent overfitting, ML learning methods and pipelines can employ several strategies. The strategy  
430 employed herein, is called nested cross-validation (nested CV), which splits the data into “training”,  
431 “validation”, and “testing” datasets. In the “inner CV loop”, the performance measures are approximately  
432 optimized by fitting a model to each of several training datasets. Subsequently, the performance measures  
433 are directly optimized by selecting hyperparameters with each validation dataset. In the “outer CV loop”,

434 the testing error is estimated by averaging test set scores for several dataset splits. In order to prevent data  
 435 leakage, it is critical that the trained models have never been exposed to the testing data.

436 When performing CV, the selection of the sizes of the training, validation, and testing sets is critical  
 437 because this choice affects the bias/variance tradeoff for a given statistical model. To strike a balance  
 438 between bias and variance error, this paper uses five folds (*i.e.*, partitions) for both the inner and outer CV  
 439 loops which can generate a favorable bias/variance tradeoff according to the literature [34]. This choice  
 440 results in 25 validation scores and 5 testing performance measure scores for each model.

### 441 **3. Datasets**

442 In this study, two datasets – field and laboratory concrete compressive strength data - are used. The field  
 443 dataset is from the Colorado Department of Transportation (CDOT); it has 1681 mixture designs and  
 444 corresponding compressive strength values. The mixture constituent variables in this dataset include  
 445 masses of cement, fly ash, water, water-reducing admixtures (WRA), coarse aggregate, fine aggregate,  
 446 and percent air entrainment. The laboratory dataset was obtained from the Machine Learning Repository  
 447 at the University of California, Irvine [35]. This dataset contains over 1000 mixture designs and  
 448 corresponding compressive strength values. However, it originally contained some mixtures that included  
 449 blast-furnace slag (a mixture ingredient not included in the field dataset) as well as some mixtures in  
 450 which the compressive strength was measured earlier than 28 days of curing. In order to reconcile these  
 451 differences, only mixtures that do not include blast furnace slag and that measure compressive strength  
 452 after 28 days are included in this analysis. This decision reduced the number of usable mixtures to 311.  
 453 One last discrepancy is that the laboratory dataset does not report air entrainment values. It is not clear  
 454 which of the following is true: a constant amount of air was entrained, no air was entrained, or variable  
 455 amounts of air were entrained but not reported. Notably, this discrepancy does not prevent model training  
 456 for either dataset. However, when the best laboratory predictive model is used to predict field  
 457 compressive strength, the air entrainment predictor cannot be utilized.

458  
 459 Table 1 provides a statistical summary of the two datasets. The laboratory dataset has been converted  
 460 to US customary units for ease of comparison. Note also that both datasets have used the Absolute  
 461 Volume Method for proportioning concrete mixtures, which generates weights of ingredients on a cubic  
 462 yard basis; this means that ingredient quantities are comparable between datasets.

463  
 464 **Table 1.** Statistical summary of laboratory- and field-acquired datasets.

Dataset	Statistic	Cement	Fly Ash	Coarse Aggregate	Sand	Water	Air	WRA	Strength
	Units	lbs/yd <sup>3</sup>	lbs/yd <sup>3</sup>	lbs/yd <sup>3</sup>	lbs/yd <sup>3</sup>	lbs/yd <sup>3</sup>	Vol. %	oz/yd <sup>3</sup>	psi
<b>Lab</b>	Mean	501	113	1678	1332	307	-	149	5357

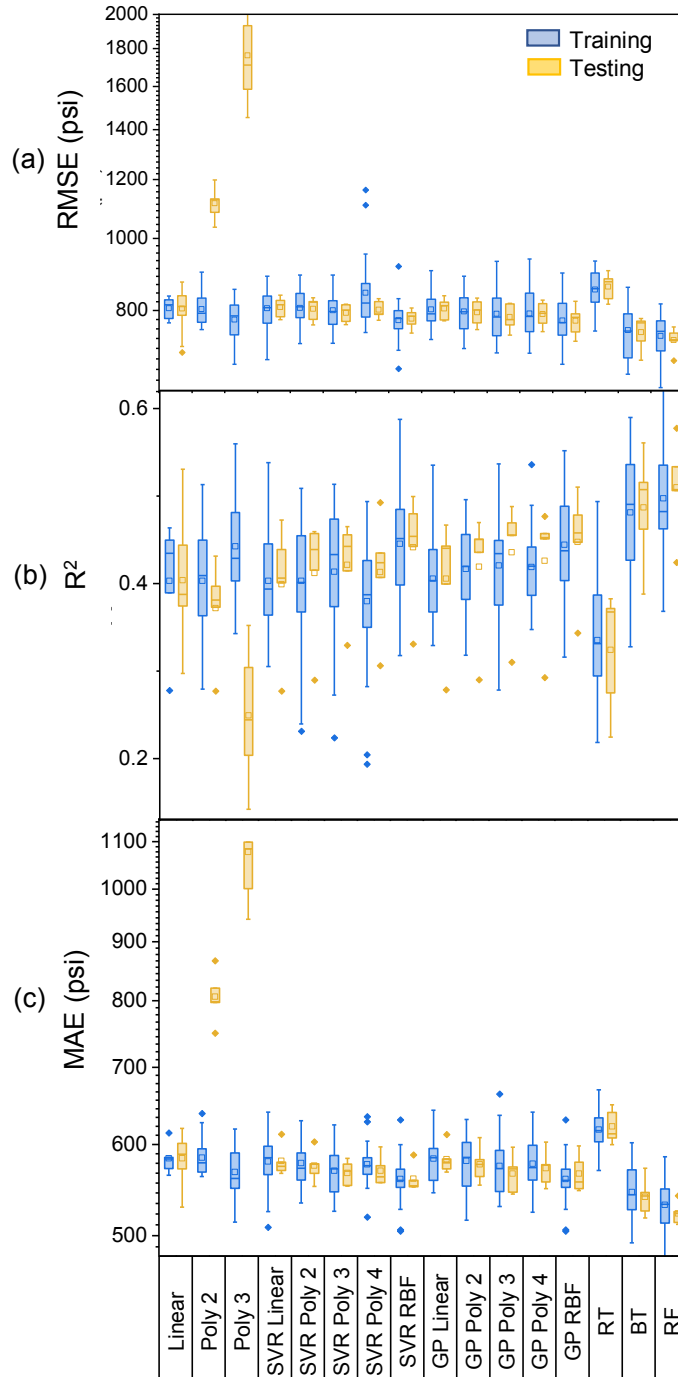
	Median	487	161	1689	1330	314	-	154	5362
	Min	227	0	1350	1001	236	-	0	1239
	Max	910.2	337	1896	1593	384	-	761	11602
<b>Field</b>	Mean	540	106	1697	1256	265	6.6	28	5938
	Median	528	120	1725	1250	265	5.8	24	5820
	Min	395	0	430	445	142	0	0	3400
	Max	900	250	2240	2250	392	9.6	305	13040

465

#### 466 **4. Results and Discussion**

467 In this analysis, we evaluate the predictive performance of the aforementioned ML models. The values for  
468 RMSE, MAE, and  $R^2$  for all models are reported in Figure 3. Low values for RMSE and MAE, and high  
469 values for  $R^2$  indicate better model performance, respectively. For simplicity of discussion, RMSE is used  
470 as the primary metric of performance. In addition, both the testing and validation performance is reported,  
471 which facilitates the discussion on overfitting in the models. These performance measures are plotted as  
472 boxplots to illustrate the range and variance of the error. The set of errors for each model is determined  
473 using a nested five-fold cross-validation, with five testing values and twenty-five training values for each  
474 model. Each model's performance from a methodological standpoint is discussed in the sections to  
475 follow. The methodological and architectural reasons for each model's performance are also examined.





476

477 **Figure 3.** Boxplots of the three cross-validated performance measures – (a) RMSE, (b)  $R^2$ , and (c) MAE  
 478 for all ML models. Both the training and testing performance measures are reported. The abbreviations  
 479 are as follows: linear regression (Linear), polynomial regression (Poly), support vector regression (SVR),  
 480 Gaussian process regression (GP), regression tree (RT), boosted tree (BT), random forest (RF). Kernels  
 481 are referred to as follows: second-order polynomial (Poly 2), third-order polynomial (Poly 3), fourth-  
 482 order polynomial (Poly 4), radial basis function (RBF).

483 *4.1 Linear Regression*

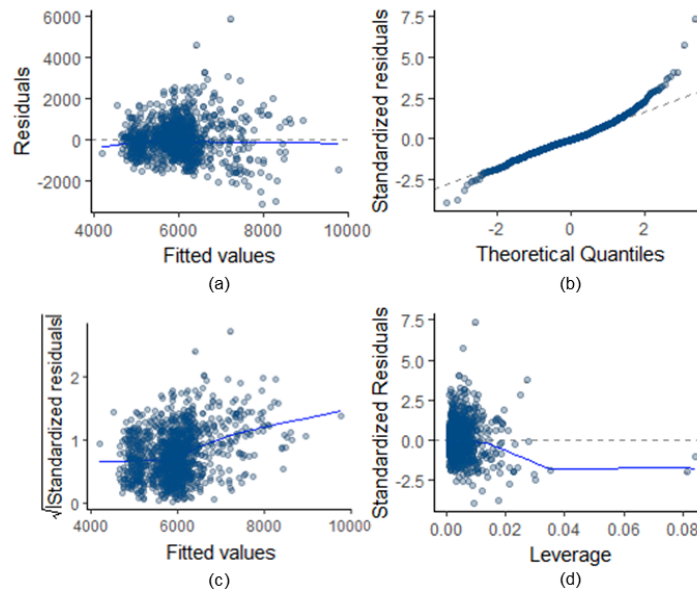
484 Linear regression is the first model tested in this analysis. This model assumes that the predictors are  
485 independent and the residuals are homoscedastic and normally distributed. The performance of linear  
486 regression is used as a baseline for comparing model performance and for determining what other models  
487 may be more appropriate for the data. For the linear regression model, Bayesian information criterion  
488 (BIC) – a parsimonious model selection criterion – is employed to select important predictor variables. Of  
489 the seven mixture ingredients, BIC selects five of these as predictor variables (cement, fly ash, water, air,  
490 and WRA); this model has a mean testing RMSE, MAE, and  $R^2$  of 803 psi, 582 psi, and 0.40,  
491 respectively. Of note is the relatively low value of  $R^2$ , which indicates that a linear model is only able to  
492 capture 40% of the variance in the data.

493 There are two possible reasons for the poor performance of this model. One reason is that there are  
494 strong predictor variables that were not measured in the dataset. Consequently, the model does not have  
495 all necessary information and is unable to perform well. A second possible reason is that the data does not  
496 fit the linear assumption of the model, that is, the assumption that the predictors are linearly to produce an  
497 output. These possibilities are further evaluated below in diagnostic plots.

498 Four diagnostic plots are shown in Figure 4. Figure 4a shows a plot of the residuals versus the  
499 predicted outputs; significant deviation of the smoothed red line indicates non-constant error variances  
500 and outliers. For this model, the smoothed average of the error variances indicates nearly constant error  
501 variance. The quantile-quantile (Q-Q) plot (Figure 4b) diagnoses the normality of the residuals. Normal  
502 residuals (in the statistical sense) lie along the dotted line; however, this figure indicates that there is some  
503 deviation from normality of the residuals among higher residual values. Figure 4c is a scale-location plot,  
504 which illustrates whether the homoscedasticity assumption is violated. For this plot, the residuals are  
505 standardized (to have a mean of zero and a variance of one) and the absolute value is taken. This plot  
506 shows that there is a slight increase in error variance with increasing compressive strength, which is  
507 indicative of minor heteroscedasticity. Lastly, Figure 4d shows the standardized residuals against their  
508 leverage, which is helpful for indicating if particular points more strongly influence the regression. In this  
509 case, a few outlier points more highly influence the regression. However, the figure also plots contours of  
510 the Cook's distance measure, which measures the effect of deleting a given observation. Cook's distance  
511 is increased by both leverage and large residuals. Since no points have a Cook's distance greater than 0.5,  
512 there is no great concern about large residuals also having too great of leverage over the fit.

513 One conclusion from the model diagnostics is that there are only minor assumption violations (non-  
514 normality of residuals and heteroscedasticity). Despite this result, the linear model retains poor predictive  
515 performance, which indicates that there are unmeasured variables needed for predicting compressive

516 strength. Nevertheless, it is reasonable to investigate the use of other types of models to determine if  
517 improved performance can be achieved.



518

519 **Figure 4.** Model diagnostic plots: **(a)** Residuals versus predicted plot to check for non-constant error  
520 variance for both positive and negative residuals, **(b)** Quantile-quantile plot to check normality of  
521 residuals, **(c)** Scale-location plot to inspect homoscedasticity, and **(d)** Residuals versus leverage plot to  
522 determine if any outliers severely impact the regression equation. The blue lines represent the smoothed  
523 average for each model diagnostic.

#### 524 4.1.1 Polynomial Regression

525 Polynomial regression introduces higher order terms and interaction terms between variables, which can  
526 sometimes improve model performance because they approximate unobserved phenomena. Here, the  
527 polynomial regression has potential because the linear regression analysis indicates a lack of the  
528 necessary predictors for improving model performance. In this analysis, polynomial regression is  
529 employed for second order and third order terms to determine if there is a physical basis for higher order  
530 variables or interaction terms.

531 One key aspect of polynomial regression is that the method acts like a feature selection method. In  
532 other words, a set of polynomial features is created, and then the features with the largest reduction in  
533 RMSE are kept for the final model. This is the method by which interaction terms are discovered. During  
534 the experiments in this paper, the following terms were discovered and included in the model:

535  $(Water) \times (WRA) \times (Air)$  and  $(Cement)^2 \times (Fly\ ash)$ . The first feature is somewhat intuitive; it is  
536 expected that some interaction between water and WRA would be relevant. However, it is somewhat less  
537 intuitive that air content is also a part of this feature. The second feature is intuitive because it is expected

538 that fly ash and cement would interactively have an impact on concrete compressive strength.  
539 Promisingly, polynomials of order two and three decrease the *training* RMSE compared to the linear  
540 model by 2.0% and 2.8%, respectively. Given this trend, it's likely that the RMSE of this model will  
541 decrease given unlimited computational power.

542 However, it is critical to also analyze the testing error. The testing error values for polynomial orders  
543 two and three are higher than the training error by 40.6% and 123.8%. This result suggests that the  
544 polynomial regression models are too flexible and overfit the data as the polynomial order grows. Thus  
545 this model type is not suitable for compressive strength prediction in concrete.

#### 546 *4.2 Kernel Transformations and Regression*

547 A different approach to discovering interactions and modeling unobserved phenomena is to use non-linear  
548 transformations of the data. Some of these are commonly known as kernel transformations. This section  
549 will survey techniques in using kernel transformations.

##### 550 **4.2.1 Support Vector Regression**

551 Solving the regression problem using kernel transformations, support vector regression is a popular  
552 technique that has shown good results in the literature. In this paper, an array of kernels was tested in  
553 cross-validation. These kernels include the RBF kernel, and polynomial kernels (2, 3, and 4).

554 One of the major goals of adaptive regression techniques like SVR is to discover any underlying structure  
555 in the data. Of the tested kernels, the RBF kernel has the greatest reduction in RMSE compared to linear  
556 regression. Here, RBF SVR reduces the average RMSE by 2.9%. In contrast, the linear and polynomial  
557 kernels (orders 2, 3, and 4) reduce this error by -0.6%, -0.1%, 1.1%, and 0.2%, respectively.

558 From this result, it is inferred that the RBF kernel generates the optimal hyperplane for linearly separable  
559 patterns among the tested kernels. The minimal improvement from polynomial kernels implies that the  
560 regression curve is not well-modeled by a polynomial.

561 The performance of SVR with RBF demonstrates that transformation of the predictor variables  
562 improves upon the linear regression baseline model. However, as will be demonstrated in section 3.3,  
563 further improvements in performance can be made with other models. One possible explanation for this  
564 behavior is that SVR can suffer from the curse of dimensionality in the sense that all terms in the  
565 transformed space are given equal weight, so the kernel cannot adapt itself to focus on the critical  
566 “subspaces” of the data [34]. Hastie et al. illustrates this concept via a prediction problem with four  
567 standard normal features (*i.e.*, “real” features) with a polynomial decision boundary and six Gaussian  
568 random features (*i.e.*, “noise” features) [34]. Although applying a polynomial kernel with SVR reduces  
569 the test error, the real features are drowned out by the noise features. In the example, kernelized SVR is  
570 unable to perform as well compared to when the real features are the only modeled features. We  
571 hypothesize that this behavior is also true in this case; the noise of irrelevant variables essentially

572 overpowers the predictive capability of SVR to capture the true underlying behavior of field compressive  
573 strength.

#### 574 **4.2.2 Gaussian Process Regression**

575 As is displayed in Figure 3 the GP training and testing performance show that the RBF kernel also  
576 generates the highest performance for GP for the kernels utilized in this study. Compared to the linear  
577 regression baseline, the GP with RBF-transformed data decreases the average testing RMSE by 3.6%.  
578 Utilizing the linear and polynomial (orders 2, 3, and 4) transformations, the reduction in RMSE is -0.1%,  
579 1.0%, 2.5%, and 1.6% respectively. With these results, we can conclude that the same transformation  
580 (RBF) generates the hyperplane most suitable for use in both SVR and GP.

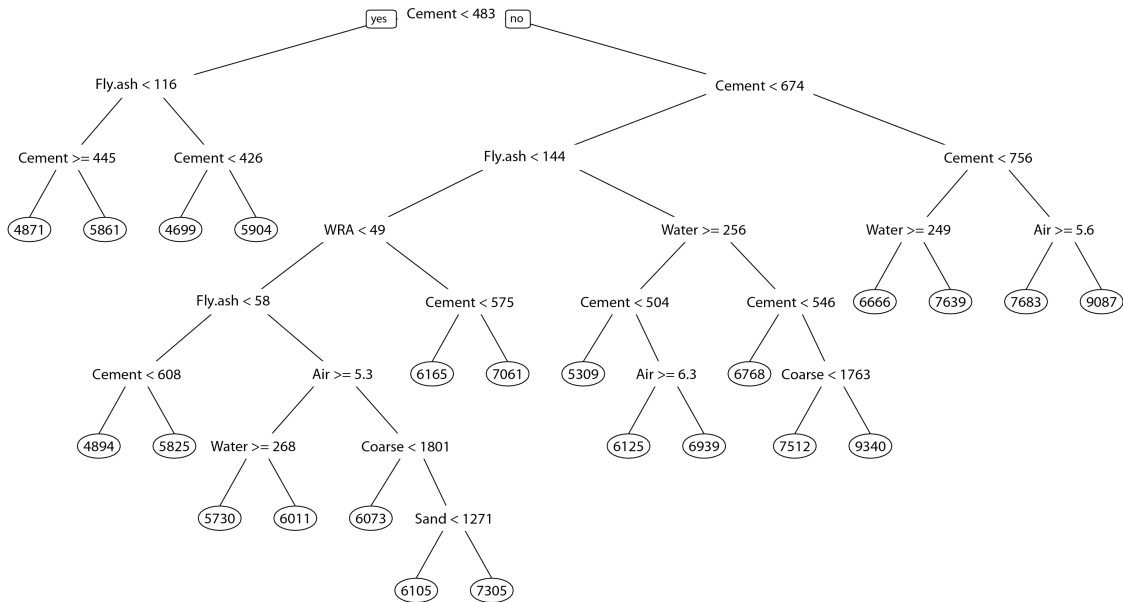
581 Moreover, this analysis shows that GP is preferred over SVR for this type of data due to its improved  
582 performance measures. We hypothesize that GP is a better-performing method (compared to SVR) due to its  
583 further relaxation of the linearity assumption. Unlike GP, SVR retains the assumption that a  
584 transformation of the predictor space causes the data to be linearly separable. GP, on the other hand,  
585 makes predictions based on the maximum likelihood of an output given the data, normal parameter  
586 distributions, and penalty term that minimize the prediction error. The improved performance of GP over  
587 SVR indicates that model performance improves when no linearity assumption exists.

### 588 *4.3 Tree-based Models*

#### 589 **4.3.1 Simple Regression Trees**

590 Unlike the aforementioned techniques, tree-based methods assume that the predictor variables may be  
591 partitioned repeatedly and that each final partition generates a different output value. For the simplest  
592 tree-based method (regression trees), the average testing RMSE indicates an increase of 6.9% compared  
593 to linear regression. We hypothesize that this result is due to the instability of regression trees. In other  
594 words, the constructed nodes for a tree may change significantly if the input training sample is slightly  
595 changed. Figure 3 illustrates the decreased performance of this model for all three metrics: RMSE,  
596 MAPE, and  $R^2$ .

597 Although the testing performance of the simple regression tree indicates it should not be used for  
598 prediction, the results of the model can be used to better understand the relative importance of certain  
599 variables for determining concrete compressive strength. In Figure 7, the nodes (e.g. Cement < 569 lbs.)  
600 and terminal node predictions (e.g. 4868 psi) are illustrated in the regression tree graph. Values of cement  
601 are the first and second nodes, as well as multiple nodes lower in the tree, which indicate the importance  
602 of cement quantity as a discriminating predictor variable for this tree. The next most important variable is  
603 the quantity of fly ash, which, like cement, has positive correlation with strength. All of the mixture  
604 ingredients appear in nodes in the tree, indicating that all are valuable for prediction.



605

606 **Figure 5.** This figure represents the best-performing simple regression tree graph for compressive  
 607 strength prediction. Final predictions from each terminal node are in shown in ellipses.

608 **4.3.2 Boosted Trees**

609 Boosted methods are used to reduce the instability of single trees. In this paper, the ensemble tree model  
 610 reduced the average testing RMSE by 13.2% compared to the simple regression tree and by 6.9%  
 611 compared to linear regression. For this dataset, boosted trees are the second best method for prediction  
 612 based on the three performance measures. Notably, the average training RMSE for boosted trees (749 psi)  
 613 is slightly lower than that of the random forest model (751 psi). However, the random forest model has  
 614 the lower testing RMSE by 5.4%. Despite the nested cross-validation routine, it appears that the boosted  
 615 tree model is slightly overfitted due to the higher value of testing RMSE compared to the training RMSE.  
 616 Recall from section 2.1.6, that this method iteratively builds regression trees on the residuals from each  
 617 consecutive tree. We hypothesize that the model has learned noise in the residuals rather than signal in the  
 618 data, which has lead to lower testing performance.

619 **4.3.3 Random Forest**

620 Like boosted trees, the random forest model reduces the instability of simple regression trees by utilizing  
 621 an ensemble of trees that utilize bootstrap aggregation and random variable selection. Consequently, the  
 622 model decreases the average testing RMSE by 9.4% compared to the linear model. It also improves upon  
 623 the testing RMSE of the simple regression tree by 20.0%. Furthermore, the average testing error is  
 624 slightly lower than the average validation error (730 psi versus 739 psi) indicating that it is unlikely that

625 the random forest model is overfitted. These testing and validation performance measures indicate that  
626 random forest is the best method for predicting compressive strength with this dataset. It has the lowest  
627 RMSE and MAE as well as the highest  $R^2$  value (730 psi, 530 psi, and .51, respectively).

628 This result may be due to the ability of tree-based methods to learn inconsistent variable importance in  
629 the data. In other words, each tree, trained on a subset of the data might learn a slightly different set of  
630 variable importance weights. In aggregate, the random forest can then better predict the target variable.  
631 An example of inconsistent variable importance can be seen in Figure 5; for mixtures with cement  
632 quantities of less than 569 pounds, the next most important variable for determining strength is fly ash. In  
633 contrast, above 569 pounds, the next splitting criterion is an even higher quantity of cement. Not only do  
634 random forest models have the ability to learn inconsistent variable importance, they also reduce the  
635 instability of individual trees and reduce the potential for overfitting [47].

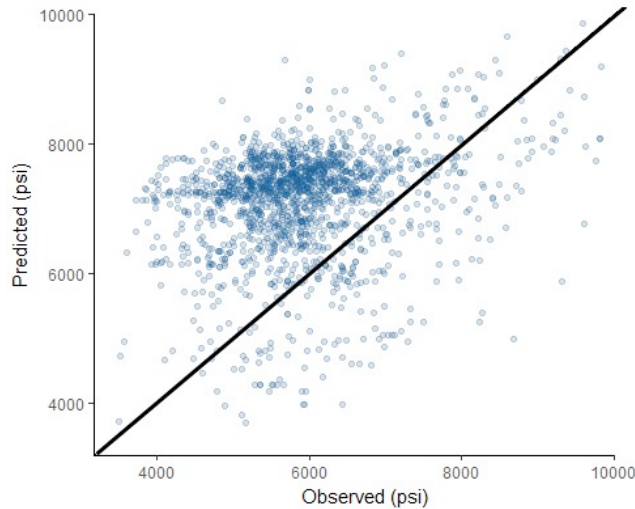
#### 636 *4.4 Prediction of Field Compressive Strength with Laboratory and Hybrid Models*

##### 637 **4.4.1 Models Trained on Laboratory Data**

638 As was discussed in Section 2, many studies in the literature have developed ML models for predicting  
639 concrete compressive strength using laboratory datasets. While these laboratory models report high  
640 predictive performance, it is relevant to consider whether they are useful for predicting field concrete  
641 strength.

642 Consequently, in this study, a suite of ML models (*i.e.*, linear regression, polynomial regression,  
643 kernel regression, tree-based models) is trained and tested using the laboratory data described in Section  
644 3. Among those tested, the highest-performing model for the laboratory dataset is the random forest  
645 model, in which the number of random variables selected at each node was 3, and the number of trees was  
646 550 trees; this model achieves a testing  $R^2$  value of 0.80.

647 Subsequent to the random forest model selection, the predictor variables from the field data have been  
648 used as inputs in the laboratory random forest model to determine how well the model can predict  
649 compressive strength of real concrete. The predicted output is plotted versus the observed field strength  
650 value in Figure 6. Points near the 1:1 line would indicate a high-performing model. This plot shows that  
651 despite its high performance using laboratory data, the laboratory model is not able to predict field  
652 strength to a high degree of accuracy; the RMSE for the field data is 1655 psi. Furthermore, this plot  
653 illustrates that, overall, the laboratory model tends to over-predict compressive strength. It is likely that  
654 this effect is due to the ideal curing conditions in the laboratory setting, which would tend to generate  
655 higher compressive strength values than if the same mixture was cured under highly variable  
656 environmental conditions.



657

658 **Figure 6.** Predicted versus observed plot for field compressive strength predictions using the random  
 659 forest laboratory model, which illustrates the models tendency to overpredict strength.

#### 660 4.4.2 Models Trained on Hybrid Data

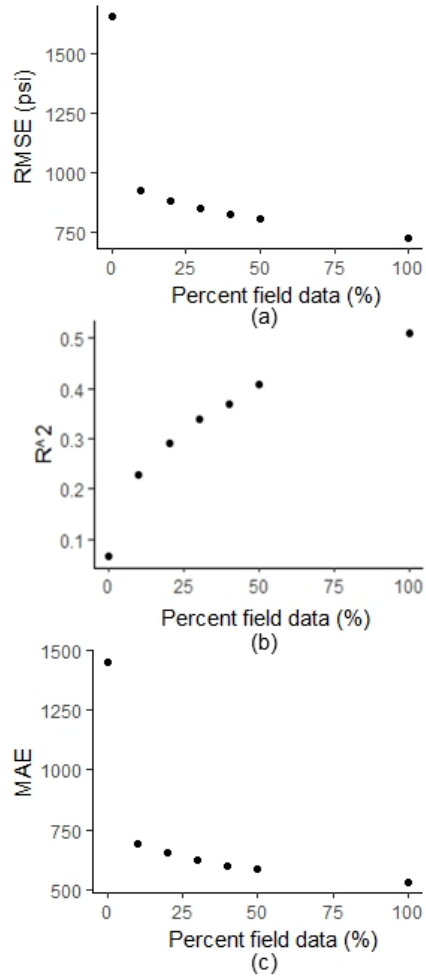
661 As was described in Section 2.3.2, models employing hybrid training data are explored in order to  
 662 determine if small amounts of field data can improve the performance of laboratory ML models for  
 663 predicting compressive strength of field concrete. In this analysis,  $\alpha$  values of 10%, 20%, 30%, 40%, and  
 664 50% replacement percentages are selected via the quintile sampling method discussed in section 2.3.2.  
 665 The remaining, unused field data is to determine the average testing performance of each hybrid model.

666 As was hypothesized, the inclusion of small percentages of field data significantly reduces the RMSE  
 667 MAE and increases the  $R^2$  (compared to a pure laboratory model). As is shown in Figure 7, the most  
 668 significant model improvements occur with the addition of the initial 10% of field data, which reduces the  
 669 RMSE by 43.0%. However, continued performance improvements occur with the additional  
 670 supplementation of field data driving the models. Furthermore, Figure 8 illustrates via predicted vs.  
 671 observed scatter plots how the addition of field data improves predictive performance. A model  
 672 comprised of 100% field data, which was analyzed in Section 4.3, is the standard with which the hybrid  
 673 models are compared in terms of the extent to which predictive performance could be improved. This  
 674 analysis illustrates that ML modeling of hybrid training data is a promising area of research that improves  
 675 upon the downsides of field models and laboratory models being used in isolation.

676 Future research in this area may explore different ML methods (*i.e.*, models other than random forest)  
 677 or other hybridization strategies for utilizing hybrid training data. In addition, it may be of interest to  
 678 focus this modeling procedure on concretes with exotic mixture ingredients, which inherently have been  
 679 rarely employed in industry, and thus, have few data points with which to model compressive strength.

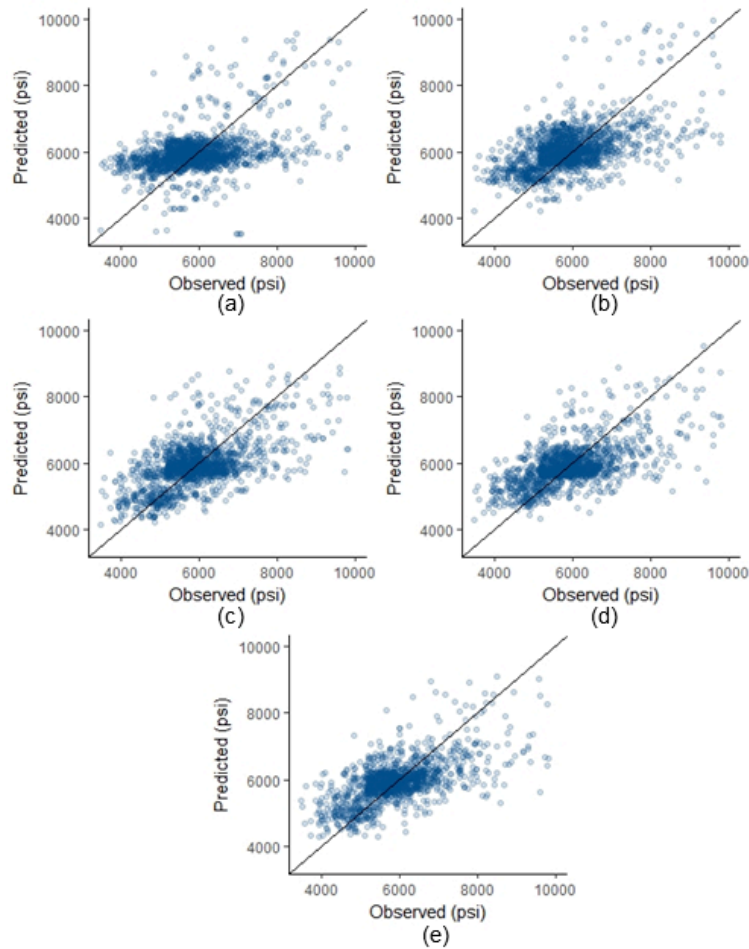
680





681

682 **Figure 7.** Graphs illustrating the continued improvement in (a) RMSE, (b) R<sup>2</sup>, and (c) MAE as additional  
 683 field data is supplied to the model.



684

685 **Figure 8.** Scatter plots of predictive versus observed for ML models trained on hybrid data with the  
 686 following percentages of field data: **(a)** 10%, **(b)** 20%, **(c)** 30%, **(d)** 40%, **(e)** 50%. Points lying near the  
 687 one-to-one line indicate better model performance.

688 **5. Conclusions**

689 The goal of this work was to specifically analyze the compressive strength behavior of *field concrete* as a  
 690 function of mixture ingredient quantities. Furthermore, this work trained and tested a variety of ML  
 691 models for predicting compressive strength of field concrete mixtures and determined which ML models  
 692 are best suited for the data. By analyzing the performance measures and a variety of diagnostic plots, the  
 693 reasons for differing performance for field concrete ML models have been elucidated. For instance, from  
 694 the linear regression model diagnostics, it was found that there are only very minor violations of linearity  
 695 assumptions; this result indicated it is likely that important predictor variables are missing from the data.  
 696 Further manipulation of the predictor space via polynomial regression and kernel transformation indicated  
 697 that a transformed predictor space can improve predictive capability (via a 4% reduction in testing  
 698 RMSE). Moreover, it was found that nonlinear models, specifically random forest, generated the best

699 performance measures, which is attributed to its full rejection of linear assumptions and ability to learn  
700 inconsistent variable importance in the data.

701 It was also confirmed that, at the current time, the most accurate prediction of compressive strength of  
702 field concrete is achieved with models trained on field concrete data; however, ML models that employ  
703 hybrid training data show promise for significantly improving predictive performance of laboratory  
704 concrete models even when only small amounts of field concrete data are available. For instance, it was  
705 found that, when only 10% of the training data were from field concrete, the RMSE was reduced by 43%.  
706 Moving forward, this research could be extended to explore other ML models with the hybridized  
707 approach or applications when it is desirable to explore modeling of exotic concrete mixtures and  
708 ingredients.

709 Broadly, the results of this research support two main conclusions: (1) Prediction of field concrete  
710 strength requires the application of nonlinear ML models using field-specific data. In particular, advanced  
711 tree-based models, such as random forest, are the highest-performing, even when field data is relatively  
712 less abundant than laboratory data. (2) Although there is value in testing and statistical-model training for  
713 the strength prediction of laboratory concrete, these models should not be used for stand-alone prediction  
714 of field concrete strength, because they do not capture the many convoluting factors of field concrete  
715 placement and curing. However, ML models that employ hybrid training data can significantly improve  
716 the predictive performance compared to laboratory concrete ML models that are used in isolation.

717

## 718 **6. Acknowledgments**

719 This research was made possible by the Department of Civil, Environmental, and Architectural  
720 Engineering, the College of Engineering and Applied Sciences, and the Living Materials Laboratory at  
721 the University of Colorado Boulder, with support from the National Science Foundation (Award No.  
722 CMMI-1562557). This work represents the views of the authors and not necessarily those of the sponsors.

723

## 724 **References**

- 725 [1] ACI Committee 318, “Building code requirements for reinforced concrete,” American Concrete  
726 Institute, ACI 318, 2014.
- 727 [2] M. Alshihri, A. Azmy, and M. El-Bisy, “Neural networks for predicting compressive strength of  
728 structural light weight concrete,” *Constr. Build. Mater.*, vol. 23, no. 6, pp. 2214–2219, 2009.
- 729 [3] A. Oztas, M. Pala, E. Ozbay, E. Kanca, N. Caglar, and M. A. Bhatti, “Predicting the compressive  
730 strength and slump of high strength concrete using neural network,” *Constr. Build. Mater.*, vol. 20,  
731 no. 9, pp. 769–775, 2006.

- 732 [4] C. Bilim, C. D. Atiş, H. Tanyildizi, and O. Karahan, "Predicting the compressive strength of ground  
733 granulated blast furnace slag concrete using artificial neural network," *Adv. Eng. Softw.*, vol. 40, no.  
734 5, pp. 334–340, May 2009.
- 735 [5] H.-G. Ni and J.-Z. Wang, "Prediction of compressive strength of concrete by neural networks,"  
736 *Cem. Concr. Res.*, vol. 30, no. 8, pp. 1245–1250, Aug. 2000.
- 737 [6] J. Zhang and Y. Zhao, "Prediction of Compressive Strength of Ultra-High Performance Concrete  
738 (UHPC) Containing Supplementary Cementitious Materials," in *2017 International Conference on  
739 Smart Grid and Electrical Automation (ICSGEA)*, 2017, pp. 522–525.
- 740 [7] S.-C. Lee, "Prediction of concrete strength using artificial neural networks," *Eng. Struct.*, vol. 25,  
741 no. 7, pp. 849–857, Jun. 2003.
- 742 [8] S. Akkurt, S. Ozdemir, G. Tayfur, and B. Akyol, "The use of GA-ANNs in the modelling of  
743 compressive strength of cement mortar," *Cem. Concr. Res.*, vol. 33, no. 7, pp. 973–979, Jul. 2003.
- 744 [9] I. B. Topcu, "Prediction of properties of waste AAC aggregate concrete using artificial neural  
745 network," *Comput. Mater. Sci.*, vol. 41, no. 1, pp. 117–125, 2007.
- 746 [10] U. Atici, "Prediction of the strength of mineral admixture concrete using multivariable regression  
747 analysis and an artificial neural network," *Expert Syst. Appl.*, vol. 38, no. 8, pp. 9609–9618, Aug.  
748 2011.
- 749 [11] M. Rguig and M. El Aroussi, "High-Performance Concrete Compressive Strength Prediction Bsed  
750 Weighted Support Vector Machines," *Int. J. Eng. Res. Appl.*, vol. 7, no. 1, pp. 68–75, Jan. 2017.
- 751 [12] B. G. Aiyer, D. Kim, N. Karingattikkal, P. Samui, and P. R. Rao, "Prediction of compressive  
752 strength of self-compacting concrete using least square support vector machine and relevance vector  
753 machine," *KSCE J. Civ. Eng.*, vol. 18, no. 6, pp. 1753–1758, 2014.
- 754 [13] C. Deepa, K. Sathiya Kumari, and V. Pream Sudha, "Prediction of the compressive strength of high  
755 performance concrete mix using tree based modeling," *Int. J. Comput. Appl.*, vol. 6, no. 5, pp. 18–  
756 24, 2010.
- 757 [14] D. A. Abrams, "Water-Cement Ratio as a Basis of Concrete Quality," *J. Proc.*, vol. 23, no. 2, pp.  
758 452–457, Feb. 1927.
- 759 [15] S. Popovics, "Analysis of Concrete Strength Versus Water-Cement Ratio Relationship," *Mater. J.*,  
760 vol. 87, no. 5, pp. 517–529, Sep. 1990.
- 761 [16] M. S. Mamlouk and J. P. Zaniewski, *Materials for Civil and Construction Engineers*, 2nd ed. Upper  
762 Saddle River, NJ: Pearson Education, Inc., 2006.
- 763 [17] R. Kozul, "Effects of Aggregate Type, Size, and Content on Concrete Strength and Fracture  
764 Energy," University of Kansas Center for Research, Inc., Lawrence, KS, SM Report No. 43, 1997.

- 765 [18] A. Fernández-Jiménez and A. Palomo, "Characterisation of fly ashes. Potential reactivity as alkaline  
766 cements☆," *Fuel*, vol. 82, no. 18, pp. 2259–2265, Dec. 2003.
- 767 [19] A. A. Ramezani-pour and V. M. Malhotra, "Effect of curing on the compressive strength,  
768 resistance to chloride-ion penetration and porosity of concretes incorporating slag, fly ash or silica  
769 fume," *Cem. Concr. Compos.*, vol. 17, no. 2, pp. 125–133, Jan. 1995.
- 770 [20] J. Fox, "Fly Ash Classification - Old and New Ideas," presented at the 2017 World of Coal Ash  
771 Conference, Lexington, KY, 2017.
- 772 [21] A. M. Zeyad, "Effect of curing methods in hot weather on the properties of high-strength  
773 concretes," *J. King Saud Univ. - Eng. Sci.*, May 2017.
- 774 [22] O. Cebeci, "Strength of concrete in warm and dry environment," *Mater. Struct.*, pp. 270–272, 1987.
- 775 [23] B. A. Young, A. Hall, L. Pilon, P. Gupta, and G. Sant, "Can the compressive strength of concrete be  
776 estimated from knowledge of the mixture proportions?: New insights from statistical analysis and  
777 machine learning methods," *Cem. Concr. Res.*, Sep. 2018.
- 778 [24] M. A. DeRousseau, J. R. Kasprzyk, and W. V. Srubar, "Computational design optimization of  
779 concrete mixtures: A review," *Cem. Concr. Res.*, vol. 109, pp. 42–53, Jul. 2018.
- 780 [25] I.-C. Yeh, "Optimization of Concrete Mix Proportioning Using Flattened Simplex-Centroid Mixture  
781 Design and Neural Networks," *Eng. Comput.*, vol. 25, no. 179, pp. 179–190, 2009.
- 782 [26] M. Pala, E. Özbay, A. Öztaş, and M. I. Yuce, "Appraisal of long-term effects of fly ash and silica  
783 fume on compressive strength of concrete by neural networks," *Constr. Build. Mater.*, vol. 21, no. 2,  
784 pp. 384–394, Feb. 2007.
- 785 [27] G. Trtnik, F. Kavčič, and G. Turk, "Prediction of concrete strength using ultrasonic pulse velocity  
786 and artificial neural networks," *Ultrasonics*, vol. 49, no. 1, pp. 53–60, Jan. 2009.
- 787 [28] İ. B. Topçu and M. Sarıdemir, "Prediction of compressive strength of concrete containing fly ash  
788 using artificial neural networks and fuzzy logic," *Comput. Mater. Sci.*, vol. 41, no. 3, pp. 305–311,  
789 Jan. 2008.
- 790 [29] Y. Ayaz, A. F. Kocamaz, and M. B. Karakoc, "Modeling of compressive strength and UPV of high-  
791 volume mineral-admixed concrete using rule-based M5 rule and treemodel M5P classifiers,"  
792 *Constr. Build. Mater.*, vol. 94, pp. 235–240, 2015.
- 793 [30] C. Videla and C. Gaedicke, "Modeling Portland Blast-Furnace Slag Cement High-Performance  
794 Concrete," *Mater. J.*, vol. 101, no. 5, pp. 365–375, Sep. 2004.
- 795 [31] F. Khademi, S. M. Jamal, N. Deshpande, and S. Londhe, "Predicting strength of recycled aggregate  
796 concrete using Artificial Neural Network, Adaptive Neuro-Fuzzy Inference System and Multiple  
797 Linear Regression," *Int. J. Sustain. Built Environ.*, vol. 5, no. 2, pp. 355–369, Dec. 2016.

- 798 [32] M. Sarıdemir, "Prediction of compressive strength of concretes containing metakaolin and silica  
799 fume by artificial neural networks," *Adv. Eng. Softw.*, vol. 40, no. 5, pp. 350–355, May 2009.
- 800 [33] E. Güneyisi, M. Gesoğlu, Z. Algın, and K. Mermerdaş, "Optimization of concrete mixture with  
801 hybrid blends of metakaolin and fly ash using response surface method," *Compos. Part B Eng.*, vol.  
802 60, pp. 707–715, Apr. 2014.
- 803 [34] T. Hastie, R. Tibshirani, and J. Friedman, *The Elements of Statistical Learning: Data Mining,  
804 Inference, and Prediction, Second Edition*, 2nd ed. New York: Springer-Verlag, 2009.
- 805 [35] "UCI Machine Learning Repository: Concrete Compressive Strength Data Set." [Online].  
806 Available: <https://archive.ics.uci.edu/ml/datasets/Concrete+Compressive+Strength>. [Accessed: 19-  
807 Dec-2017].
- 808 [36] "R: The R Project for Statistical Computing." [Online]. Available: <https://www.r-project.org/>.  
809 [Accessed: 06-Nov-2018].
- 810 [37] G. A. F. Seber and A. J. Lee, *Linear Regression Analysis*. John Wiley & Sons, 2012.
- 811 [38] T. Hofmann, B. Scholkopf, and A. Smola, "Kernel Methods in Machine Learning," *Ann. Stat.*
- 812 [39] H. Drucker, C. J. Burges, L. Kaufman, A. J. Smola, and V. N. Vapnik, "Support Vector Regression  
813 Machines," *Adv. Neural Inf. Process. Syst.* 9, pp. 155–161.
- 814 [40] C. Strobl, J. Malley, and G. Tutz, "An introduction to recursive partitioning: rationale, application,  
815 and characteristics of classification and regression trees, bagging, and random forests," *Psychol.  
816 Methods*, vol. 14, no. 4, pp. 323–348, Dec. 2009.
- 817 [41] L. Breiman, *Classification and Regression Trees*. Routledge, 2017.
- 818 [42] P. Probst, M. Wright, and A.-L. Boulesteix, "Hyperparameters and Tuning Strategies for Random  
819 Forest," *ArXiv180403515 Cs Stat*, Apr. 2018.
- 820 [43] J. Friedman, T. Hastie, and R. Tibshirani, "Additive logistic regression: a statistical view of  
821 boosting (With discussion and a rejoinder by the authors)," *Ann. Stat.*, vol. 28, no. 2, pp. 337–407,  
822 Apr. 2000.
- 823 [44] J. H. Friedman, "Greedy function approximation: A gradient boosting machine.," *Ann. Stat.*, vol. 29,  
824 no. 5, pp. 1189–1232, 200110.
- 825 [45] T. Chai and R. R. Draxler, "Root mean square error (RMSE) or mean absolute error (MAE)? –  
826 Arguments against avoiding RMSE in the literature," *Geosci. Model Dev.*, vol. 7, no. 3, pp. 1247–  
827 1250, Jun. 2014.
- 828 [46] P. N. Chatur, A. R. Khobragade, and D. S. Asudani, "Effectiveness evaluation of regression models  
829 for predictive data-mining," *Int. J. Manag. IT Eng.*, vol. 3, no. 3, pp. 465–483, Oct. 2013.
- 830 [47] L. Breiman, "Random Forests - Random Features," University of California, Berkeley, CA,  
831 Technical Report 567, Sep. 1999.